Songklanakarin J. Sci. Technol.
42 (2), 292-298, Mar. - Apr. 2020

http://www.sjst.psu.ac.th

Original Article

Self-potential and 2-D resistivity application for groundwater exploration in fractured reservoirs

Muhammad Taqiuddin Zakaria, Nordiana Mohd Muztaza*, Adeeko Tajudeen Olugbenga, Rosli Saad, and Muhammad Nazrin A Rahman

Geophysics Section, School of Physics,
Universiti Sains Malaysia, Gelugor, Penang, 11800 Malaysia

Received: 13 April 2018; Revised: 6 November 2018; Accepted: 12 December 2018

Abstract

The high demand for various uses of water related to domestic and industrial requirements is increasing rapidly. Alternative water supplies with less pollution and more economic value are needed to support the demand. The self-potential and 2-D resistivity methods were used to identify the flow pathways of the water and potential groundwater zones in Johor, Malaysia by measurement of the potential difference between two non-polarizable copper electrodes and resistivity distribution of the subsurface. The recharge zone of the aquifer was identified with negative potential values (0 to –140 mV) while positive values (0 to 140 mV) showed the discharges zones for this area. The self-potential results showed the flow pathways of groundwater in the direction of southeast to northwest of the study area. A potential groundwater zone was identified at resistivity values of <100 Ωm at depths >50 m. The high contrast of resistivity values indicated a fracture/fault for this area.

Keywords: self-potential, 2-D resistivity, surface water, groundwater

1. Introduction

Geophysical methods are rapid, non-destructive, relatively inexpensive, and can vastly improve the characterization of the shallow subsurface. Self-potential (SP) is one of the non-invasive geophysical methods that measures the natural potential of the Earth (Nyquist & Osiensky, 2002). The method is an established geophysical method that has been applied for various applications and research, such as mineral explorations, oil well logging, geothermal explorations, hydrogeological surveys, and many other applications within the scope of the environmental studies and engineering. The electrical method has been used widely in monitoring the groundwater occurrence within fractured rock. Fractures in rock are important pathways for groundwater flow and contaminant migration. The rate and direction of groundwater flow at a given location is driven by a hydraulic gradient which is also determined by the strength of recharge and discharge. The topography and fractures influence the groundwater flow path directions. The flow pathways follow the direction of the strike and topography toward a local stream. The groundwater flow is classified into three components: down the hydraulic gradient, downdip, and along the strike (Fan, Toran, & Schlische, 2007). Adjacent boreholes can be monitored with the application of one of the primary techniques such as a pumping test (Domenico & Schwartz, 1997) because it gives an excellent measurement of fluid flow and transport properties as hydraulic transmissivity of an aquifer. However, due to heterogeneity of a fractured rock system with a greater volume it may be impossible to extrapolate with a single measurement. The SP approach generally measures the electric potential which occurs naturally in the ground surface and the technique can be used to identify a groundwater flow path in a large scale. SP occurs below the soil surface and is caused by electrokinetic or streaming potential produced by fluid and heat fluxes in the ground, diffusion potentials across boundaries between regions of different chemical composition, and redox reactions around orebodies and buried metallic objects (Fritjof & Graham, 2003). Generally, the streaming of water through porous material and fractures in the subsurface

*Corresponding author
Email address: mmnordiana@usm.my

produces an electrical potential gradient, known as streaming potential along the flow path (Birch, 1993, 1998; Doussan, Jouniaux, & Thony, 2002; Maineult, Bernabe, & Ackerer, 2005). The potential difference fluctuates due to variation in the electric current of the ground. A negative SP anomaly is associated with a recharge area or downward flow of the water movement while positive anomalies are indicated by the strong lateral flow of water movement (Bogoslovsky & Ogilvy 1973; Leonard, Cyril, & Anthony, 2010; Ogilvy, Ostrovskij, & Ruderman, 1989).

In addition, the pioneer of resistivity sounding and profiling technique gives a 1-D model of the subsurface which is not appropriate in mapping the geological structures of higher complexity. The 2-D resistivity model provides more realistic information and visualization of the subsurface where the resistivity varies in vertical and horizontal directions along the survey lines. The values are mapped even in the presence of complex geological condition and topography (Loke, 1997 a). Recently, the 2-D resistivity method was successfully used in subsurface exploration in various environments including bedrock detection, geological mapping, and groundwater exploration (Hsu, Yanites, Chin Chen, & Chen, 2010; Rao, Prasad, & Reddy, 2013; Zhou, Matsui, & Shimada, 2004). The high demands in various types of water consumption are related to the domestic and industrial sectors such as agricultural, factory, and public supply which have increased rapidly. Thus, alternative water supplies, such as groundwater, are needed to support the current demands and provide more economic and less pollution compared to other water resources. However, a tube well at a suitable location for extracting the maximum amount of water should be chosen wisely based on consideration of the geological conditions and other parameters. A wrong decision in the selection of a suitable location may result in inefficient production in terms of cost, time, and productivity. A groundwater assessment using the geophysical approach is required to meet these challenges in determining the potential groundwater zones. In this research, the SP method was applied using 2-D resistivity for imaging the flow of groundwater in an area in Johor, Malaysia area (Figure 1).

2. Background Theory

An electrokinetic potential is produced as an electrolyte passes through a porous or capillary slit and the potential is measured along the capillary. The potential

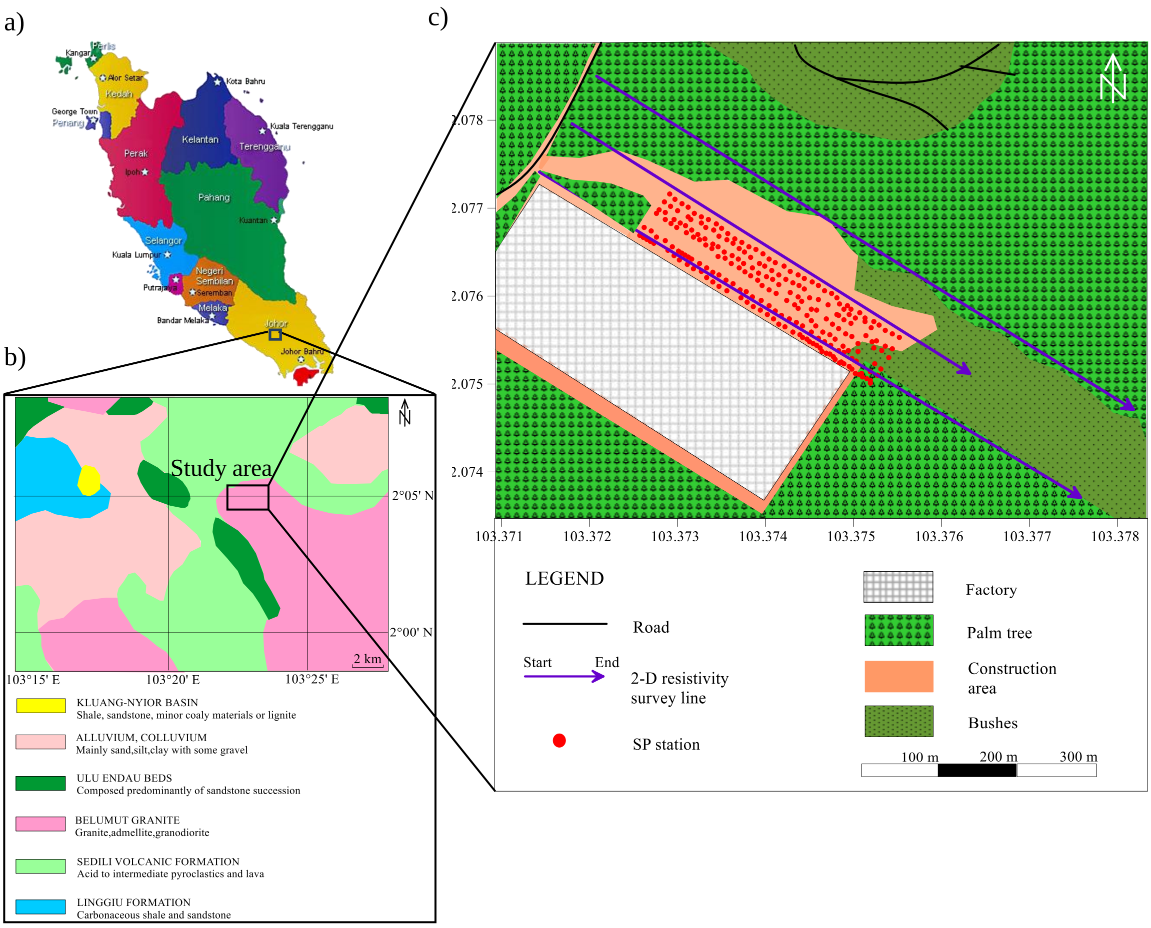

Figure 1. a) Map of Malaysia, b) Geological map of the study area, c) Map of study area (planar view).

generated from this phenomenon is categorized as a streaming potential which can be expressed in Equation 1:

$$E_K = \frac{\varepsilon\rho C_E \partial P}{4\pi\eta} \quad (1)$$

where

E_K = electrokinetic potential
ε = dielectric permittivity of pore fluid
ρ = electrical resistivity of pore fluid
η = dynamic viscosity of pore fluid
δP = the change of pressure
C_E = coupling coefficient of electrofiltration

C_E represents the physical and electrical parameters of the electrolyte as it passes through the medium. The movement of the fluid generates a potential gradient along the flow path due to the interaction between pore fluid movement and an electrical double layer which is known as the streaming potential.

The 2D resistivity method utilizes direct current to investigate electrical properties of subsurface by measuring resistivity distribution of the materials. Fluvial, lacustrine sediments, bedrock, and structural features such as faults exhibit a large contrast in resistivity values (Asry, Samsudin, Yaacob, & Yaakub, 2012). The electrical resistivity of the materials depends on the combination of ohmic and dielectric effects related to the lithology of the subsurface (Edwin & Cahit, 1988). The fundamental theory of 2-D resistivity is related to the Ohm's Law which can be expressed as;

$$\rho_a = k\frac{V}{I} \quad (2)$$

where

ρ_a = apparent resistivity
k = geometric factor of the electrode array
V = voltage
I = current

The k-values play an important role in determining the depth of investigation for 2-D resistivity surveys. The electrical resistivity of sediments and rocks is a function of porosity, saturation, the resistivity of pore fluids and solid phase, and the material structure. It was observed in many cases that in water-bearing rocks the resistivity varies as the inverse square of the porosity. Archie's law (Archie, 1942) describes how resistivity depends on the porosity of the rock and conductivity of the pore fluid.

3. Methodology

3.1 Study area and geological setting

The study area (Figure 1c) was located in Johor, Malaysia where it is generally covered by Tertiary sediment similar to Batu Arang and other Tertiary basins of West Malaysia, and similar to the Late Tertiary age (Staufer, 1973a). In addition, Burton in 1964 reported the possibility of a Quarternary age for these sediments while considering the nonconformity of the overlying alluvium in the Early Pleistocene or Pliocene age. Figure 1b shows the rock unit of the study area is granite, adamellite, and minor granodiorite from Belumut granite (Kia *et al.,* 2012). The units showed various dip directions of the sediments and the rapid changes in the lateral thickness and depth compared to the older rocks, i.e. granite and volcanic rocks. The shallow depth sediments area is composed of sand clay, clay, sand, and shale while the deeper geology is made up of granite, volcanic rock, tuff, and quartzite. A previous facies analysis on the outcrop done by previous geologists showed that the lithology outcrops were mostly light-coloured which may indicate the lack of decomposed organisms (carbon) within them. Furthermore, the layers were also not fully consolidated sandstone that ranged from medium grain to coarse grain with a wide range of grain sizes. The dominant mineral present was quartz followed by feldspar (Meng, Jamin, Mohamed, & Mun, 2016). The sediment was deposited in a fluvial environment which included a floodplain and abandoned channel predominantly made up of mudstone, siltstone, and sandstone. Most of the mudstone and siltstone that were rich in organic materials were light grey to dark grey in colour (Said, Rahmah, Hamid, & Ariffin, 2003). The area was mostly low-land surrounded by hills with different elevations.

3.2 Field procedure

3.2.1 Self-potential (SP)

The SP method uses two non-polarizable copper electrodes and two porous pots with an ABEM SAS300 Terrameter for data acquisition. The copper electrodes were suspended in a supersaturated solution of copper sulphite (Cu SO_4) inside a porous container. One of the electrodes is used as a fixed reference called the base station and is located outside the survey lines. The location of the base is carefully selected with uniform streaming potential to reduce telluric and cultural noises for better data accuracy. Since the $CuSO_4$ is sensitive to temperature changes (1.2 mV/°C) (Jardani, Dupont, & Revil, 2006), it is important to reach thermal equilibrium between the porous pot and the surrounding soil before starting the measurements. The P_1 pole (negative terminal) at the ABEM SAS300 was connected to the base electrode while the P_2 pole (positive terminal) was attached to a rover electrode. The base station reading was repeated every two hours after the measurement of the rover station for a drift correction. To obtain the highest consistency reading, the holes of each station were dug deeply enough to penetrate the surface soil with intervals for of each station ranging from 3–5 m. SP was measured as the difference in electric potential between the reference electrode (base station) and another electrode (rovers). Measurements of the data were done three times and four different values were given for each measurement. A 3-min time interval was allowed before each repetition of data measurements after placing the electrodes (rovers) on the ground. The data was taken in three repetitions to improve the signal-to-noise ratio. In data processing, Surfer8 software was used for mapping and contouring the data to produce a residual SP map.

3.2.2 2-D resistivity

In the 2-D resistivity survey, the ABEM SAS4000 with the pole-dipole array and 5 m minimum electrode spacing system were used to acquire the data. The pole-dipole array was chosen since the array can give a greater penetration depth with good data resolution. Three survey lines were designed in such a way to fulfil the objective of the study. The lines are L1, L2, and L3 with a distance of 800 m, 600 m, and 800 m respectively. The survey used 41 electrodes during each measurement and they were connected to a multichannel cable and ES10-64C electrode selector for the data measurement. The roll-along technique was applied in certain cases by extending the data measurement with overlapping of 50 m for each next spread of acquisition. The resistivity data were processed in Res2dinv software for an inversion model and Surfer8 software for interpretation and correlation. The results obtained are presented in a 2-D resistivity inversion model where the range of resistivity values are indicated by a color scale

4. Results and Discussions

4.1 SP

The SP data presented in Figures 2a and 2b were obtained using the Kriging algorithm for contouring and interpolation of data. Surfer8 software was used to optimize and smooth the data. SP anomalies are associated with the presence of water in subsurface structures and the flow of water pathways through the ground (Jinadasa & Silva, 2009). In this survey, the electrochemical sources were neglected in the interpretation because the study area has no indication of significant oxidation or reduction reactions associated with biodegradation of solid waste materials such as leachate or contaminated water flow. The thermoelectric effect, which is related to temperature variations, was also neglected since it showed minor contribution to the data. The observed SP field is considered to be created primarily by electrokinetic sources which are related to the fluid flow in the subsurface. The magnitude of the potential field is inversely proportional to the electrolytic concentration of the pore fluid; hence, the maximum contribution of the SP anomaly is generated by the flow of freshwater (Bogoslovsky & Oglivy, 1973). In this study, the potential values ranged from –140 mV to 140 mV (Figure 2a). The interpretation of the SP data was based on the water flow path according to the values. The contour revealed a spatially non-uniform distribution over the study area where a distinguishable positive anomaly with a high anomaly was located at the edge of the map. The first anomaly was a large positive SP zone near the reference electrode that increased positively towards the northwest of the map. This positive anomaly was suspected as groundwater discharge at the base of a steep slope (Corwin & Hoower, 1979). The second anomaly was the SP zone with the highest negative values and it was located at the edge of the northwest direction which represented the recharge area. In the map, low potential values from –140 mV to positive values were distributed at the southwest part of the map. A streaming potential of groundwater is usually indicated by a negative anomaly of the profile (Colangelo, Lapenna, Perrone, Piscitelli & Telesca, 2006). Negative SP anomalies are normally associated with the downslope movement of the subsurface water (Corwin, 1990; Panthulu, 2001). The location was considered to have a slight topographic depression (Figure 2b) which could indicate a lateral variation in material properties or vertically descending flow of bedrock fault or fracture zone. An SP distribution associated with steep topography was examined and reported by previous researchers and it showed signs relative to shallow groundwater flow (Corwin & Hoover, 1979; Ernston & Scherer, 1986). This study showed accumulation of surface water which had flowed to this region. The magnitude of the direction showed the movement of the water and the high magnitude indicated a rapid flow of the water in the area. Other than that, the water discharging and charging activities for this area were considered to actively occur due the wide range of potential values.

4.2 2-D resistivity

The 2-D resistivity data are presented in a 2-D inversion model of resistivity. The position of the first electrode location was corrected and the filtered data were inverted using a least squares inverse technique with smoothness constraints and the Gauss-Newton optimization technique using Res2Dinv (Loke, 1997a; Loke, 1997b). The calculated apparent resistivity values of the model block were compared with the measured apparent resistivity values. It was adjusted

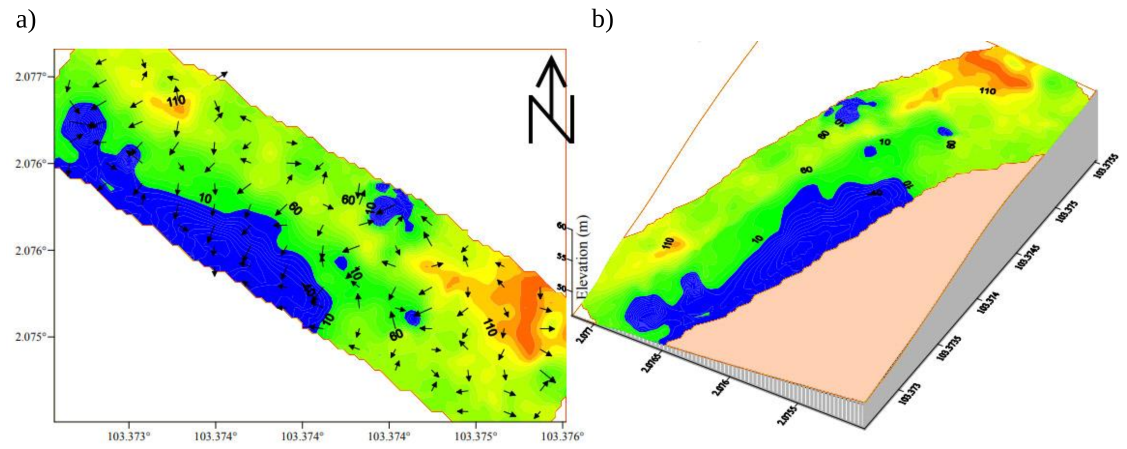

Figure 2. Self-potential contour map (planar view), b) Self-potential contour map with topography.

Table 1. Summary of the results.

Method	Values/Anomaly	Descriptions
Self-potential	Positive anomaly (0 to140 mV)	Associated with groundwater discharge
	Negative anomaly (0 to −140 mV)	Associated with groundwater recharge
2-D Resistivity	<100 Ωm	Saturated zone (Potential groundwater)
	>700 Ωm	Cap layer for the aquifer
	Contrast zone	Presence of fracture/fault

iteratively until the values of the model achieved high closeness with the measured apparent resistivity values. A root mean square value less than 35% was observed, which indicated a high similar model block to the apparent resistivity.
Figure 3a shows the 2-D resistivity inversion model of L1 with resistivity values that ranged from 1 to 10000 Ωm and a depth of investigation of 150 m. From this model, the saturated zone was identified with resistivity values <100 Ωm at depths >50 m. This zone was classified as the potential groundwater zone. The low resistivity values, at the top layer of the profile along a distance of 0–350 m indicated the accumulation of surface water and this was closely agreeable with the SP results. The contrast zone was interpreted as a fracture /fault (black dashed lines) which may act as a potential pathway for the groundwater to seep upward due to the difference in pressure gradient. High resistivity values >700 Ωm indicated the cap layer for the aquifer. The 2-D resistivity model in Figure 3b shows the continuation of profile L1. The subsurface features were identified as the fracture/fault zone at depths >50 m due to the contrast in the resistivity values. Several isolated zones of low resistivity values (1–100 Ωm) were associated with a saturated weathered layer. A resistivity region of >700 Ωm was classified as the cap layer for the aquifer at depths >50 m. A low resistivity region at depths <50 m was associated with the water movement from the sur-face which had accumulated in the region. Figure 3c shows the 2-D resistivity inversion model of L3 with the depth investigation at 150 m. The result of this profile showed good correlation between lines L1 and L2 as low regions of resisti-vity at depths <50 m which indicated percolation of surface water at a distance of 0–300 m. The region with resistivity values <100 Ωm indicated a saturated zone for the aquifer at depths >50 m.

In addition, the saturated zones for all three profiles of L1–L3 showed resistivity values <100 Ωm, which possibly indicated the presence of clay and sand with the correlation of geological setting of the area. According to Telford (1990),

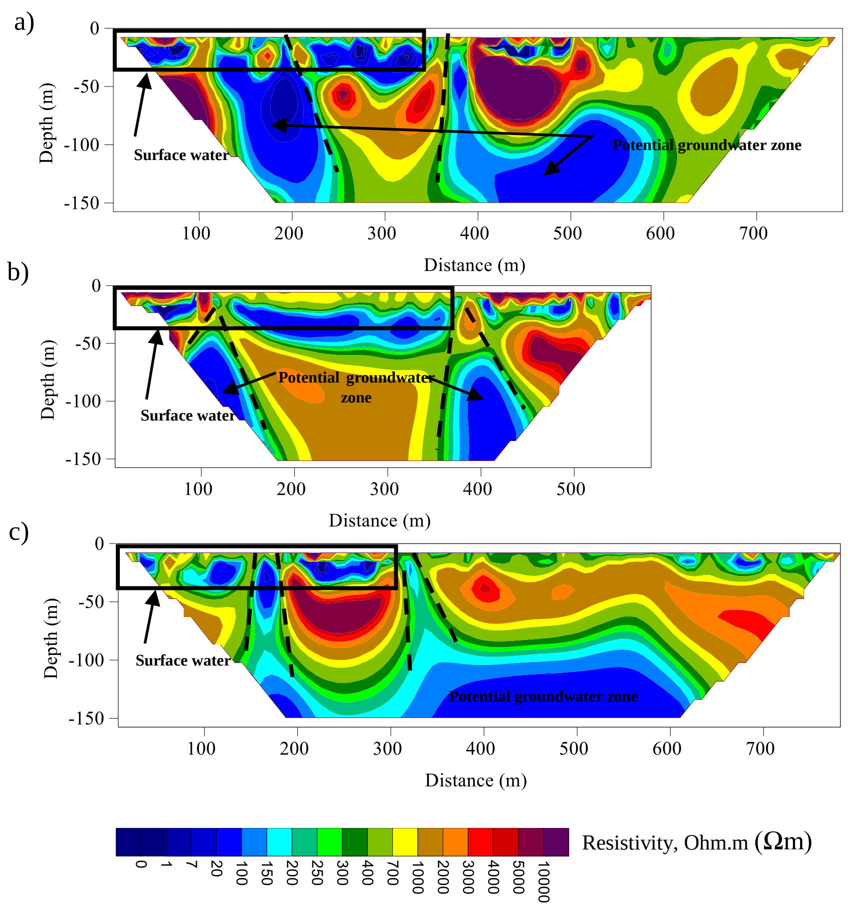

Figure 3. 2-D resistivity inversion model: a) L1; b) L2; and c) L3

the resistivity values for clay vary from 1 to 100 Ωm which agreed with Abidin, Saad, Ahmad, Wijeyesekera, and Baharuddin (2014). The authors stated that the resistivity values for water at the surface and natural conditions vary from 1 to 100 Ωm. The presence of clay and other finer sediments enhance the subsurface material in retaining the water from migrating due to porosity and permeability factors. This phenomenon results in low resistivity values of the materials compared to coarser soil such as sand or gravel which tends to produce high resistivity values. Finer sediments with fine grain sizes, such as clay soil, consist of high mineral compositions of kaolinite and illite which causes the current to flow easier with less resistance which results in low resistivity values (Abidin *et al.,* 2017). The variation in resistivity values is due to several factors, such as the concentration and types of iron within the pore fluid and the grain matrix which influences the rate at which the current is carried by the mineral irons (Grifith & King, 1981). Other than that, in sand/gravel formations the resistivities values range from 40 to 400 Ωm that represent potential groundwater zones (Ismail, Schwarz, and Pederson, 2011). The resistivity values are inversely proportional to water content and dissolved ion concentration (Liu & Evett, 20 08). A saturated zone is caused by fractures in the hard rock which allows the water to seep through and trap inside it. Low resistivity values are associated with a great degree of fracturing (Loke, 1997a). Therefore, the low resistivity values for this locality indicated a saturated zone which could be classified as a confined aquifer. Resistivity values that ranged from 700 to 3000 Ωm in this locality were interpreted as the presence of sandstone. Fractures play an important role in controlling the secondary porosity of the reservoir (Warren & Root, 1963). Generally, secondary porosity is due to mechanical processes such compaction, deformation, and fracturing (Schön, 2015).

5. Conclusions

The flow of the water was successfully defined with the correlation of self-potential and 2-D resistivity methods. The result of 2-D resistivity was used to confirm the ambiguity that arises in SP interpretation. From the SP results of the study area, the flow pathways of the groundwater were determined to be from the southeast to the northwest. Negative potential values, i.e. 0 to −140 mV, were identified as the accumulation zone of the surface water as it moves due to the potential gradient, while positive potential values (0 to 140 mV) represented the discharge zone of the study area. According to the 2-D resistivity results, the subsurface characteristics of the profile lines showed that the surface water was identified at depths <50 m, meanwhile at depths >50 m, the saturated zone with resistivity values of <100 Ωm was classified as the potential groundwater zones. A low resistivity region was associated with water movement from the surface which accumulated in the region. The high contrast in resistivity values showed the presence of a fracture/fault line with several isolated zones of low resistivity values (1–100 Ωm) associated with the saturated weathered layer. The correlation of both results showed the accumulation of the surface water which flows to this region as water discharging. The water recharging activity for this area is considered to actively occur due to the wide range of potential values.

Acknowledgements

The author wishes to thank, all lecturers, staff personnel, and postgraduate students from the geophysics section Universiti Sains Malaysia (USM) for their assistance during the geophysical data acquisition. The author wishes to thank USM for providing the Research University Grant entitled Geophysical Application and Approaches in Engineering and Environmental Problems (1001/PFIZIK/811323) and Fundamental Research Grant Scheme entitled Development of 2-D Linear Inversion Algorithm from Geophysical Approach for Soil or Rock Characteristics. Special thanks are also extended to the USM Fellowship for providing the tuition funding.

References

Abidin, M. H. Z., Raqib, A. G. A., Aziman, M., Azhar, A. T. S., Khaidir, A. T. M., Fairus, Y. M., . . . Izzaty, R. A. (2017). Prelimanary groudwater assessment using electrical method at quaternary deposits area. *IOP Conference Series: Materials Science and Engineering*, *226*, 1-11.

Abidin, M. H. Z., Saad, R., Ahmad, F., Wijeyesekera, D. C., & Baharuddin, M. F. T. (2014). Correlation analysis between field electrical resistivity value and basic geotechnical properties. *Soil Mechanics and Foundation Engineering*, *51*, 117-125.

Archie, G. E. (1942). The electrical resistivity log as an aid in determining some reservoir characteristics. *Transactions of the AIME*, *146*(01), 54-62.

Asry, Z., Samsudin, A. R., Yaacob, W. Z., & Yaakub, J. (20 12). Groundwater investigation using electrical resistivity imaging technique at Sg. Udang, Melaka, Malaysia. *Bulletin of the Geological Society of Malaysia*, *58*, 55–58.

Birch, F. S. (1993). Testing Fournier's method for finding water table from self-potential. *Ground Water*, *31*, 50–56.

Birch, F. S. (1998). Imaging the water table by filtering self-potential profiles. *Ground Water*, *36*, 779–782.

Bogoslovsky, V. A., & Oglivy, A. A. (1973). Deformation of natural electric fields near drainage structures. *Geophysical Prospecting*, *21*, 716-723.

Burton, C. K. (1964). The older alluvium of Johore and Singapore. *Journal Tropical Geography*, *18*, 30-42.

Colangelo, G., Lapenna V., Perrone A., Piscitelli, S., & Telesca, L. (2006). 2D Self-Potential tomographies for studying groundwater flows in the Varco d'Izzo landslide (Basilicata, southern Italy). *Engineering Geology*, *88*(3-4), 274-286.

Corwin, R. F. (1990). The self-potential method and engineering applications. *Geotechnical and Environmental Geophysics*, *1*, 127-146.

Corwin, R. F., & Hoover, D. B. (1979). The self-potential method in geothermal exploration. *Geophysics*, *44*, 226 –245.

Domenico, P. A., & Schwartz, F. W. (1997). *Physical and Chemical Hydrogeology* (2^{nd} ed.). Hoboken, NJ: John Wiley and Sons.

Doussan C., Jouniaux L., & Thony J. L. (2002). Variations of selfpotential and unsaturated water flow with time in sandy loam and clay loam soils. *Journal*

Hydrology, *267*, 173–185.

Edwin, S. R., & Cahit, C. (1988). *Basic Exploration Geophysics*. New York, NY: John Wiley and Sons.

Ernstson, K., & Scherer, H. U. (1986). Self-potential variations with time and their relation to hydrogeologic and meteorological parameters. *Geophysics*, *51*(10), 1967–1977.

Fan, Y., Toran, L., & Schlische, R. W. (2007). Groundwater flow and groundwater-stream interaction in fractured and dipping sedimentary rocks: Insights from numerical models. *Water Resources Research*, *43*, W01409.

Fritjof, F. & Graham, H. (2003). Detecting subsuraface groundwater flow in fractured rock using sel-potential (SP) methods. *Environmental Geology, 43*, 782-794.

Griffith, D. H., & King, R. F. (1981). *Applied geophysics for geologist and engineers.* Oxford, England: Pergamon Press.

Hsu, H., Yanites, B. J., Chih Chen, C., & Chen, Y. (2010). Bedrock detection using 2D electrical resistivity imaging along the Peikang river, central Taiwan. *Geomorphology*, *114*, 406-414.

Ismail, N., Schwarz, G., & Pedersen, L. B. (2011) Investigation of groundwater resources using controlled source radiomagnetotelluric (CSRMT) in glacial deposits in Heby, Sweden. *Journal of Applied Geophysics, 73*, 74 – 83

Jardani, A., Dupont, J. P., & Revil, A. (2006). Self-potential signals associated with preferential groundwater flow pathways in sinkholes. *Journal of Geophysical Research*, *3*, 4-13.

Jinadasa, S. U. P., & Silva, R. P. (2009). Resistivity imaging and self-potential applications in groundwater investigations in hard crystalline rocks. *Journal of the National Science Foundation of Sri Lanka*, *37*(1), 23-32.

Kia, M. B., Pirasteh, S., Pradhan, B., Mahmud, A. R., Sulaiman, W. N. A., & Moradi, A. (2012). An artificial neural network model for flood simulation using GIS: Johor River Basin, Malaysia. *Environmental Earth Sciences*, *67*(1), 251-264.

Leonard, I. N., Cyril, N. N., & Anthony, S. E. (2010). Correlation of self-potential and resistivity survey methods for evaluation of groundwater potentials: Case study of Imo State, Nigeria, *Applied Physics Research*, 3 (1), 100-109.

Liu, C., & Evett, J. B. (2008). *Soils and foundations* (7^{th} ed.). Upper Saddle River, NJ: Pearson Prentice Hall.

Loke, M. H. (1997a). Electrical imaging surveys for environmental and engineering studies. A practical guide to 2-D and 3-D surveys. Retrieved from https://pdfs.semanticscholar.org/efa9/43ffb44f5a217e2d22255f7e334778932248.pdf?_ga=2.246136580.1479738836.1575556606-1618557801.1572104258

Loke, M. H. (1997b). RES2DINV. 2D interpretation for DC resistivity and IP for windows 95 [Computer software]. Penang, Malaysia: Geotomo Software.

Maineult, A., Bernabe´, Y., & Ackerer, P. (2005). Detection of advected concentration and pH fronts from self-potential measurements. *Journal of Geophysical Research*, *110*(B11). doi:10.1029/2005JB003824

Meng, C. C., Jamin, N. H. M., Mohamed, M. A., & Mun, C. S. (2017). *Sedimentology of potential tertiary fluvial deposits in Kluang, Johor, Malaysia*. International Conference on Integrated Petroleum Engineering and Geosciences 2016. Retrieved from https://www.springer.com/gp/book/9789811036491

Nyquist, J. E., & Osiensky, J. L. (2002). Self-potential: The ugly duckling of environmental geophysics. *The Leading Edge*, *21*(5), 446-451.

Ogilvy, A. A., Ostrovskij, E. J., & Ruderman, E. N. (1989). Electrical surveys using the method of the natural electric field; new investigations. In G. P. Merkler, H. Militzer, H. Hötzl, H. Armbruster, & J. Brauns (Eds.) *Detection of subsurface flow-phenomena. Lecture notes in earth sciences Vol. 27* (pp. 401-466). Berlin Berlin, Germany: Springer.

Panthulu, T. V., Krishnaiah, C., & Shirke, J. M. (2001). Detection of seepage paths in earth dams using self-potential and electrical resistivity methods. *Engineering Geology*, *59*, 281-295.

Roa, B. V., Prasad, Y. S., & Reddy, K. S. (2013). Hydrogeophysical investigations in a typical khondalitic terrain to delineate the kaolinised layer using resistivity imaging. *Journal Geological Society of India, 81*, 521-530.

Said, U., Rahmah, R. A., Hamid, A., & Ariffin M. M. M. (20 03). Early cretaceous palynomorphs from Kampung Tanah Runtuh, Kluang Johor. *Geological Society of Malaysia Bulletin, 46*, 143-147.

Schön, J. H. (2015). Pore Space Properties. *Developments in Petroleum Science*, *65*, 21-84.

Staufer, P. H. (1973). Cenozoic. In D. J. Gobbett & C. S. Hutchison (Eds.), *Geology of the Malay Peninsula* (pp. 143-176). New York, NY: Wiley-Interscience.

Telford, W. M., Geldarl, L. P., & Sheriff, R. E. (1990). *Applied geophysics*. Cambridge, England: Cambridge University Press.

Warren, J. E., & Root, P. J. (1963). The behavior of naturally fractured reservoirs. *Society of Petroleum Engineers Journal*, *3*, 245-255.

Zhou, Q. Y., Matsui, H., & Shimada, J. (2004). Characterization of the unsaturated zone around a cavity in fractured rocks using electrical resistivity tomography. *Journal of Hydraulic Research*, *42*, 25-31.